Title Page

Gene-by-Environment Interaction of Bcrp$^{-/-}$ and MCD Diet-Induced Nonalcoholic Steatohepatitis Alters SN-38 Disposition

Erica L. Toth, Hui Li, Anika L. Dzierlenga, John D. Clarke, Anna Vildhede, Michael Goedken, Nathan J. Cherrington

Department of Pharmacology and Toxicology, University of Arizona, Tucson, AZ (E.L.T, H.L., A.L.D., N.J.C), Pharmaceutical Sciences, Washington State University, Spokane, WA (J.D.C), Pharmacokinetics, Dynamics and Metabolism, Medicine Design, Pfizer Worldwide R&D, Groton, CT (A.V.), Research Pathology Services, Rutgers University, Newark, NJ (M.G.)

DMD # 82081

Running Title Page

Running title: Alteration of SN-38 Disposition in Bcrp-Null NASH Rat Model

Send Correspondence To: Nathan Cherrington, PhD, Dept of Pharmacology and

Toxicology, University of Arizona, 1703 E Mabel Street, Tucson, AZ 85721 USA, Phone:

520-626-0219, E-mail: cherrington@pharmacy.arizona.edu

Number of text pages: 14

Number of tables: 0

Number of figures: 6

Number of references: 30

Number of words in abstract: 250

Number of words in introduction: 768

Number of words in discussion: 1,376

Abbreviations (alphabetical order):

ABC, ATP-binding cassette; Actb, beta actin; ADRs, adverse drug reactions; AUC, area

under the curve; BCA, bicinchoninic acid; Bcrp, breast cancer resistance protein; DTT,

dithiothreitol; HRP, horseradish peroxidase enzyme; IV, intravenous; LC-MS/MS, liquid

chromatography-tandem mass spectrometry; Mrp2, multidrug resistance protein 2;

Mrp3, multidrug resistance protein 3; NAFLD, nonalcoholic fatty liver disease; NASH,

nonalcoholic steatohepatitis; MCD, methionine-choline deficient; P-gp, P-glycoprotein;

DMD # 82081

qRT-PCR, quantitative real-time polymerase chain reaction; SIL, stable isotope labeled;

SN-38G, SN-38 glucuronide; SNPs, single nucleotide polymorphisms; SULT,

sulfotransferase; UGT, Uridine 5'-diphospho-glucuronosyltransferase; UPLC, ultra-high

performance liquid chromatography

Abstract

Disease progression to nonalcoholic steatohepatitis (NASH) has profound effects on the expression and function of drug metabolizing enzymes and transporters, which provides a mechanistic basis for variable drug response. Breast cancer resistance protein (BCRP), a biliary efflux transporter, exhibits increased liver mRNA expression in NASH patients and preclinical NASH models, but the impact on function is unknown. It was shown that the transport capacity of multidrug resistance protein 2 (MRP2) is decreased in NASH. SN-38, the active irinotecan metabolite, is reported to be a substrate for Bcrp, whereas SN-38 Glucuronide (SN-38G) an Mrp2 substrate. The purpose of this study was to determine the function of Bcrp in NASH through alterations in the disposition of SN-38 and SN-38G in a *Bcrp* knockout (Bcrp-/-) and methionine-choline deficient (MCD) model of NASH. Sprague Dawley (WT) rats and Bcrp-/- rats were fed either a methionine and choline sufficient (control) or MCD diet for 8 weeks to induce NASH. SN-38 (10mg/kg) was administered intravenously and blood and bile was collected for quantification by liquid chromatography-tandem mass spectrometry (LC-MS/MS). In Bcrp-/- rats on the MCD diet, biliary efflux of SN-38 decreased to 31.9% and efflux of SN-38G decreased to 38.7% of control, but WT-MCD and KO-C were unaffected. These data indicate that Bcrp is not solely responsible for SN-38 biliary efflux, but rather implicates a combined role for BCRP and MRP2. Furthermore, the disposition of SN-38 and SN-38G is altered by Bcrp-/- and NASH in a gene-by-environment interaction and may result in variable drug response to irinotecan therapy in polymorphic patients.

DMD # 82081

Introduction

Adverse drug reactions (ADRs) are becoming increasingly frequent, and approximately 1 in 20 hospital patients experience an ADR in the United States(Bourgeois, Shannon, Valim, & Mandl, 2010; Stausberg, 2014). Variations in drug response can occur due to a variety of factors, including alterations to drug metabolizing enzymes and transporters. Understanding the mechanistic basis behind inter-individual variability can potentially identify at-risk populations.

Many variations in drug response can be attributed to genetic polymorphisms in genes that are responsible for the absorption, distribution, metabolism, and excretion (ADME) processes that determine the pharmacokinetics of drugs. Single nucleotide polymorphisms (SNPs) in *SLCO1B1* have been linked to increases in statin plasma concentrations as well as increases in statin-induced myopathy(Yee et al., 2018). Variations in multidrug resistance proteins have been known to influence therapeutic outcomes of anti-cancer treatments such as difluomotecan(Sparreboom et al., 2004) and doxorubicin(Lal et al., 2008). Genetic variations, however, are not the sole factor involved in variable response; alterations in response to disease pathogenesis may also affect ADME processes and contribute significantly to ADRs. Transient alterations in transporter function due to disease can alter drug disposition in a manner that closely resembles the loss of function due to genetic variations. These alterations create a phenotype that is incongruent with genotype; a phenomenon referred to as phenoconversion.

Nonalcoholic steatohepatitis (NASH) is the hepatic manifestation of metabolic syndrome. Disease progression to NASH presents with hepatocellular injury,

5

inflammation, and fibrosis(Marra, Gastaldelli, Svegliati Baroni, Tell, & Tiribelli, 2008) and

the prevalence of NASH is overall about 1.5-6.45%(Younossi et al., 2016). In addition

to the histological changes, there are also significant alterations to hepatic enzyme and

transporter mRNA, protein expression, and function that are important to ADME

processes, such as the ATP-binding cassette transporter (ABC) family(Anika L

Dzierlenga et al., 2016; R. N. Hardwick et al., 2013). A global transcriptional study

among NASH patients showed that the effect of NASH progression on transporters is a

phenoconversion event; many uptake transporters are significantly downregulated, and

efflux transporters like MRP2, MRP3, and BCRP are significantly upregulated(Lake et

al., 2011). Both MRP2 and BCRP are members of the ABC family and are located on

the bile canaliculus of the liver, where they efflux endo- and xenobiotics. MRP3 is an

ABC transporter located on the sinusoidal membrane, where it transports compounds

back into the blood. Mislocalization of MRP2 during NASH significantly decreases its

function(Anika L Dzierlenga et al., 2016), and alterations to the MRP2/MRP3 transport

system can result in significantly altered drug disposition such as the increase in plasma

retention of pemetrexed in rodent models of NASH(Anika L Dzierlenga et al., 2016).

mRNA analyses of human NASH liver tissue has also shown an increase in *BCRP*

expression during the disease(R. N. Hardwick, Fisher, Canet, Scheffer, & Cherrington,

2011). Alterations in BCRP function have not been explored, and it is important to

understand changes to BCRP in the context of other transporters.

Irinotecan is a camptothecin-derivative chemotherapeutic that is used to treat colorectal

cancers, the third leading cause of cancer death(Siegel, Desantis, & Jemal, 2014). It

undergoes hepatic metabolism to a variety of metabolites, only one of which, SN-38, is

active. SN-38 is a known substrate of BCRP(Houghton et al., 2004; Tuy et al., 2016), and SN-38G, like many glucuronides, is thought to be mainly exported through MRP2(Kroetz, 2006). Patient response to irinotecan, however, is highly variable and carries a significant risk of life-threatening side effects(Falcone et al. 2007). Enzyme polymorphisms, such as *UGT1A1*28*, account for only a portion of this variability(Sadée & Dai, 2005).   Hepatobiliary efflux of SN-38 and SN-38G facilitates the toxic effects in the intestine(Horikawa, Kato, & Sugiyama, 2002). Additionally, SN-38G in the intestine is converted back into SN-38 by β-glucuronidase and is then reabsorbed into systemic circulation, which is vital to irinotecan therapy as it prolongs circulation time(Hasegawa et al., 2006). Given the previous data on the effects of NASH on hepatobiliary transport of xenobiotics, it was hypothesized that functional alterations of BCRP and MRP2 during NASH would alter the disposition of SN-38 and SN-38G, potentially contributing to variable response. It was postulated that alterations to BCRP during NASH would significantly alter biliary elimination of SN-38 and lead to decreased plasma concentrations; it was similarly proposed that mislocalization of MRP2 could significantly reduce biliary elimination of its substrate, SN-38G, and lead to plasma accumulation. This study aimed to determine the effect of Bcrp polymorphic loss of function and NASH alone, and in a gene-by-environment interaction, on the disposition of SN-38 and SN-38G. The observations made through comparison of these models may provide mechanistic insight into inter-individual variability, and a basis for response prediction in human NASH patients.

Materials and Methods

Reagents.

SN-38 and camptothecin were purchased from Sigma-Aldrich (St. Louis, MO), and SN-38-glucuronide was purchased from Toronto Research Chemicals (Toronto, Ontario, Canada). Urethane, UPLC–grade acetonitrile, and UPLC-grade water were obtained from Sigma-Aldrich.   Heparin was purchased from Alfa Aesar (Ward Hill, MA). ReadyScript® cDNA synthesis kit, KiCqStart™ SYBR® green qPCR with low ROX™ master mix, and PCR primers for Bcrp and β-actin (Actb) were obtained from Sigma-Aldrich. RNA Bee isolation reagent was obtained from Amsbio (Cambridge, MA).

Animals.

Male *Bcrp* knockout and wild-type Sprague-Dawley rats of at least 8 weeks of age were purchased from Horizon Discovery (Saint Louis, MO). Animals were housed in a University of Arizona Association for Assessment and Accreditation of Laboratory Animal Care–certified animal facility with a 12-hour light-dark cycle and allowed to acclimatize for at least one week before experiments. A methionine and choline deficient diet (MCD) or control diet from Dyets, Inc (Bethlehem, PA) was given *ad libitum* for 8 weeks when the animals were 16 weeks of age. After 8 weeks of diet, the animals underwent disposition studies. All handling, maintenance, care, and testing of the animals was in accordance with NIH policy, and experimental protocols were approved by the University of Arizona Institutional Animal Care and Use Committee.

SN-38 and SN-38G Disposition studies.

A stock solution of 10 mg/mL of SN-38 was prepared in DMSO. From this stock solution, a 0.8 mg/mL SN-38 co-solvent solution was prepared for injection. This solution was made by adding the SN-38 stock solution to a solution of ethanol,

propylene glycol and Tween-80, then diluting in water. The final proportion of each component was as follows: 14% ethanol, 40% propylene glycol, 3% Tween-80, 10% DMSO and 33% water. No more than 5 mL/kg of solution was administered.

Animals were anesthetized for cannulation surgery using an intraperitoneal bolus dose of urethane (1g/kg, up to 10 mL/kg in saline). In order to assess the disposition of SN-38 and SN-38G, cannulas were inserted into the jugular vein for drug and saline administration, carotid artery for blood collection, and bile duct for bile collection. Prior to dosing, blood was collected from the arterial cannula as a baseline. A bolus dose of 0.8mg/kg SN-38 was then administered intravenously over a period of 90 seconds. After drug administration, blood was collected at 2, 7, 12, 20, and 40 minutes, while bile was collected at 0, 15, 30, and 45 minutes. Terminal liver and kidney was collected at 90 minutes. A portion of collected tissue was prepared for histological analyses by fixing in 10% neutral-buffered formalin for 24 hours, then exchanging for 70% ethanol until embedded in paraffin by the University of Arizona Histology Service Laboratory. The remaining tissue was flash-frozen in liquid nitrogen for storage at -80°C. Blood was collected in heparin-coated microcentrifuge tubes and was spun down for 10 minutes at 10,000xg to separate plasma from blood cells. Plasma and bile samples were also stored at -80°C.

SN-38 and SN-38G Quantification.

Sample clean-up for blood and bile samples was performed using the Bond Elut 96 Plexa solid-phase extraction plates (Agilent, Santa Clara, CA) according to the manufacturer's protocol. 40µL of plasma and 10µL of bile were used in the sample

9

preparation process. The eluent was then evaporated to dryness and reconstituted in

120 uL of mobile phase for injection onto the LC-MS/MS. The tissue homogenates

were made from 300mg of tissue and then cleaned up via protein precipitation in a 1:3

solution of homogenate to UPLC-grade acetonitrile. The samples were vortexed and

kept on ice for 10 minutes, then centrifuged at 13,000 rpm for 10 minutes. The

supernatant was collected in a new microcentrifuge tube and evaporated to dryness.

The sample was reconstituted in 120 uL of mobile phase, centrifuged at 10,000 rpm for

5 minutes, and the supernatant was collected for injection onto the LC-MS/MS, as

previously described(Khan et al., 2005).

The method for quantification of SN-38 and SN-38G in plasma, bile, and tissue was

adapted from previously published methods(D'Esposito, Tattam, Ramzan, & Murray,

2008; Khan et al., 2005).   The Arizona Laboratory for Emerging Contaminants at the

University of Arizona provided a Waters (Milford, MA) Micromass Quattro Premier XE

tandem mass spectrometer coupled to an Acquity UPLC. The mobile phase consisted

of a gradient of water (solvent A) and acetonitrile (solvent B) with 0.1% formic acid at a

flow rate of 0.3mL/min through a Waters Acquity UPLC BEH C19 column (1.7 μm, 2.1 ×

50 mm). The mobile phase was composed of A:B 90:10 (v:v) running to A:B 10:90 (v:v)

over 1.0-6.0 minutes, then returned to A:B 90:10 over 60 seconds with two minutes of

equilibration, for a total run time of 9.0 minutes. Multiple reaction monitoring in positive

mode was used to detect SN-38 at m/z 393>349, SN-38G at m/z 569.0>393.2 and

camptothecin at m/z 349.1>305.2. The retention times for SN-38, SN-38G, and

camptothecin were 3.6 minutes, 3.1 minutes, and 3.8 minutes, respectively. Recovery

determination was done using four replicates, and the recovery in plasma and bile

respectively were: 76.3% and 86.8% for SN-38, 81.3% and 77.4% for SN-38G, and 80.6% and 81.8% for internal standard. The linear range of SN-38 and SN-38G in plasma was from 50ng/mL to 1000 ng/mL, and the range in bile was from 50ng/mL to 5µg/mL. The lower limit of quantification (LLOQ) in plasma was found to be 15ng/mL for SN-38 and 20ng/mL for SN-38G; in bile, it was found to be 20ng/mL for both SN-38 and SN-38G. Peak analysis was done in MassLynx Mass Spectrometry software and data analysis and processing was done using GraphPad Prism 5.0.

Quantitative Reverse Transcription-PCR.

RNA was isolated from liver tissue using the RNA Bee isolation reagent. Between 200-300 mg of tissue was added to 4 mL of RNA Bee and homogenized. The manufacturer's protocol was followed and the resulting RNA pellet was reconstituted in 250uL of DEPC water per 100 mg of tissue, then was stored at -80°C. RNA concentration was determined using a NanoDrop 2000 UV-visible spectrophotometer (Thermo Fisher Scientific). Final preparations of RNA had a 260/280 quality ratio between 1.6 and 1.9. cDNA was prepared from the isolated RNA using the ReadyScript® cDNA synthesis kit from Sigma-Aldrich. Each reaction well contained 1x KiCqStart™ SYBR® green master mix, 100nM of forward and reverse primers, 2µL of cDNA template, and nuclease-free water up to 20µL, run in duplicate. Reactions were run on an ABI StepOnePlus Real Time PCR system with the standard SYBR® green PCR cycling profile. Fold change was determined using the delta-delta C_T method.

Histopathology.

Paraffin-embedded liver sections were stained with hematoxylin and eosin then

examined by a board certified veterinary pathologist. Tissues were incidence and severity scored using an established rodent NASH system (Kleiner et al., 2005) with endpoints including steatosis, necrosis, inflammation, hyperplasia and biliary hyperplasia. Representative digital images were acquired. Rank-order statistical methods and one-way ANOVA were used to determine differences between groups.

IHC.

Immunohistochemistry staining was performed on formalin-fixed paraffin-embedded tissue slides. The slides were deparaffinized in 100% xylene and hydrated in 100% ethanol. Antigen retrieval was performed in boiling pH 9.0 Tris-EDTA. Endogenous peroxidases were blocked using 0.3% (v/v) H_2O_2 in phosphate buffered saline (PBS) for 20 minutes. MRP2 was stained by incubating the slides overnight at 4°C with anti-MRP2 antibody (Sigma-Aldrich, M8163), followed by the Mach 4™ staining kit protocol (Biocare Medical). Images were taken using a Leica DM4000B microscope with a DFC450 camera.

Protein Preparation.

Crude membrane fractions were obtained from liver samples. Approximately 500mg of tissue was homogenized in 5mL of cold ST buffer (Sucrose Tris buffer, 10mM tris base and 250mM sucrose with 1 Protease Inhibitor Cocktail tablet (Roche, Indianapolis, IN) per 25 ml, pH 7.5). Homogenates were centrifuged at 10,000xg for 20 minutes to remove nuclei; the supernatant was decanted into a second set of ultracentrifuge tubes. The supernatant was spun at 100,000xg for 60 minutes to pellet the membranes. Membrane pellets were rinsed with buffer before being resuspended in 200μL of buffer

and stored at -80°C. Protein concentrations were determined by BCA assay (Thermo Fisher Scientific).

Immunoblotting.

Immunoblotting for MRP2 and MRP3 was performed using crude membrane preparations. Membrane preparations (60µg/lane) were separated by SDS-Page on 7.5% polyacrylamide gels. The proteins were transferred to polyvinylidene difluoride membranes, and then blocked with 5% nonfat dry milk in Tris-buffered saline/Tween-20 for at least one hour. The membranes were probed with MRP2 (Sigma-Aldrich, M8163) or MRP3 (Santa Cruz Biotechnology, SC-5775) primary antibody at a dilution of 1:500 in 2.5% blocking solution. Image processing and analysis through the ImageJ software (National Institutes of Health, Bethesda, MD) determined relative protein density and the proteins were normalized to the housekeeping protein ERK2 (Santa Cruz Biotechnology, SC-125).

Targeted proteomic quantitation of Bcrp surrogate peptide.

Homogenization of liver tissues was done in a FastPrep 24 bead mill homogenizer (MP Biomedicals, Santa Ana, CA) with 1.4 mm ceramic beads. The ProteoExtract™ Native Membrane protein extraction kit (EMD Millipore, Billerica, MA) was used to prepare membrane fractions according to the manufacturer's protocol, and protein concentrations were subsequently determined by BCAassay (Pierce, Rockford, IL). 300 µg aliquots of membrane protein fraction were prepared in 100 mM ammonium bicarbonate with 3.7 w/v% sodium deoxycholate, and then were reduced using 6 mM dithiothreitol (DTT) for 5 minutes at 95°C. The samples were alkylated with 15 mM

iodoacetamide for 20 minutes at room temperature, protected from light. Matrix for calibration curves was obtained from human serum albumin processed under the same conditions. Protein digestion was performed over 24 hours at 37°C with a protein:trypsin ratio of 1:20. The reaction was quenched with 0.2% formic acid. Bcrp peptide labeled with a stable isotope (SIL) was added as internal standard to each sample post digestion and unlabeled peptide standard was added into the matrix samples in known concentrations. The acid-precipitated sodium deoxycholate was pelleted out of the samples by centrifugation at 16,000xg and 4°C. The supernatant was transferred to a LoBind plate (Eppendorf, Hamburg, Germany) and evaporated under nitrogen to concentrate, then reconstituted in 0.1% formic acid for injection onto the LC-MS/MS.

Peptide quantification was performed on an API-6500 triple quadrupole mass spectrometer operating in ESI mode with a Shimadzu LC-30AD interface. The mobile phase consisted of solution A, 0.1% FA in water and solution B, 0.1% FA in 90:10 acetonitrile:water set to a flow rate of 0.2 mL/min. 10 µL of sample was injected onto a Kinetex C18 core-shell column (1.7 µM, 100Å, 100 x 2.1 mm), and separation occurred along the following solvent gradient: 5.5% mobile phase B for 5 minutes, linear gradient of 5.5 to 33.3% mobile phase B over 40 minutes, hold at 33.3% for 5 minutes, wash at 100% mobile phase B for 5 minutes, then re-equilibration for 4 minutes. Multiple reaction monitoring was used to detect the analyte peptide (SSLLDVLAAR) at transition 523.1>757.5 and the SIL peptide at 528.1>767.5. The mass spectrometer settings were: 500°C source temperature, 5 kV ion spray voltage, 10eV entrance potential, 50 V declustering potential, 25 V collision energy, and 15 V collision cell exit potential. Data

14

were processed in Analyst 1.6.2 (SCIEX, Ontario, Canada) and the external peptide

calibration curve was used to determine BCRP peptide concentration in the samples.

Statistical Analyses.

All results are represented as the mean ± standard deviation (SD). Two-way ANOVA

statistical analyses with Bonferroni post-test were used to compare between control and

NASH animals of each genotype group. Each group consisted of n=3 animals, except

for KO-MCD group, which consisted of n=4.

Results

Effects of MCD diet-induced NASH on the disposition of SN-38 and SN-38G.

Hemotoxylin- and eosin-stained liver sections were examined under a light microscope

at 40x magnification for histological analysis (Fig. 1). NASH hallmarks were observed in

rats fed an MCD diet for 8 weeks, including steatosis, inflammation, necrosis, fibrosis,

and biliary hyperplasia. This is consistent with previous observations using an

established NASH scoring system and recapitulates the histological findings in human

disease(Canet et al., 2014; Kleiner et al., 2005). There was no significant interaction

between the genetic knockout and disease in the severity of NASH hallmarks, except

for fibrosis; in KO-MCD animals, fibrosis was more severe than in KO-C animals. The

effects of NASH on SN-38 and SN-38G disposition were observed over 90 minutes.

The plasma AUC of SN-38 and SN-38G showed no significant alterations between

MCD groups and their controls (Fig 2). Significant reductions in biliary efflux were seen

for SN-38 and SN-38G between the KO-C and KO-MCD groups (Fig 3 A and B). Biliary

efflux of SN-38 in the KO-MCD group decreased to 31.9% of control (from 5.59±

0.102μg/min to 1.79±0.058μg/min), and efflux of SN-38G decreased to 38.7% of control

(from 49.18±0.944μg/min to 19.15±2.04μg/min).

The hepatic and renal tissue concentrations of SN-38 and SN-38G showed high

variability and no statistically significant differences between the MCD groups and their

controls (Fig. 3 C).

Effects of MCD diet-induced NASH on Mrp2 and Mrp3 protein.

Relative protein concentrations of MRP2 and MRP3 and localization of MRP2 were

determined by Western blotting and immunohistochemistry (IHC), respectively.

Densitometric analysis was used to compare relative protein expression between

groups (Fig. 4). MRP3 increased by 10-fold in the WT-MCD group when compared to

control, and increased by 3.5-fold in the KO-MCD group when compared to control.

Protein concentrations of MRP2 remained relatively unchanged between the WT-C and

WT-MCD groups and the KO-C and KO-MCD groups. Immunohistochemical staining of

MRP2 revealed normal localization at the canalicular membrane in the control groups,

while MCD groups showed pockets of internalized staining, indicating mislocalization

consistent with previous observations(A. L. Dzierlenga et al., 2015; Anika L Dzierlenga

et al., 2016).

Effects of MCD diet-induced NASH on Bcrp.

mRNA expression of Bcrp was determined by qRT-PCR and relative protein

concentration was determined by LC-MS/MS analysis of BCRP surrogate peptide (Fig.

6). *Bcrp* mRNA increased by two-fold in the WT-MCD group when compared to its

control, while both knockout groups showed no expression. Protein expression of

BCRP increased in keeping with mRNA expression, showing a 1.6-fold increase in the MCD group when compared to controls, and no expression in the knockout groups.

Discussion

The hepatobiliary disposition of SN-38 and SN-38G is mediated by BCRP and MRP2 transport, and during NASH, alterations to BCRP function can significantly impact systemic drug exposure. It has been previously established that alterations of hepatobiliary efflux pathways can affect the distribution of xenobiotics in bile and plasma, potentially increasing patient exposure and the risk of toxicity. The MRP2/MRP3 hepatobiliary efflux pathway has been found to play a significant role in the distribution of various xenobiotics, including the chemotherapeutics pemetrexed and methotrexate, and analgesics like morphine(A. L. Dzierlenga et al., 2015; Anika L Dzierlenga et al., 2016; Ferslew et al., 2015; R. Hardwick et al., 2014). The participation of other transport proteins can also affect the distribution and toxicity of xenobiotics. Uptake transporters contribute significantly to the uptake and clearance of various drugs, including SN-38. In human patients, the hepatic uptake of ^{99m}Tc-mebrofenin (MEB), a substrate for OATP1B1 and OATP1B3, was significantly decreased in NASH due to disease-related impairment(Ali et al., 2017). *Oatp1a/1b*$^{-/-}$ mice exhibit increased SN-38 concentrations in plasma and have more pronounced neutropenia(Iusuf et al., 2014). Although hepatic uptake transporters can cause alterations in xenobiotic disposition, efflux transporters are generally considered to have the most significant impact(Köck & Brouwer, 2012). SN-38 and its metabolite SN-38G are substrates for MRP2, MRP3, and BCRP, and their disposition is significantly affected by the functional status of these transporters(Kato, Suzuki, & Sugiyama, 2002).

17

While it has been previously noted that SN-38 is a substrate for Bcrp and SN-38G is a substrate for MRP2(Chu et al., 1997; Kawabata et al., 2001), our data confirm that both compounds are substrates for both transporters. The data herein indicate that biliary efflux of SN-38 and SN-38G is unchanged either by genetic disruption of Bcrp or the NASH-related disruption of MRP2 function alone, but the combination of disease and genetic disruption significantly impedes biliary efflux.

The disposition of SN-38 and its metabolite will also be influenced by the activity of UDP-glucuronosyltransferases. UGT1A1 is one of the major isoforms responsible for the glucuronidation of SN-38(Etienne-Grimaldi et al., 2015), and variants of UGT1A1 have been shown to increase the risk of neutropenia in human patients taking irinotecan(Liu, Cheng, Kuang, Liu, & Xu, 2014). The impact of NASH on UGT expression has been explored in previous research; in human patients, there is no change in either the mRNA or protein expression of UGT1A1 in when compared to normal(R. N. Hardwick et al., 2013; Lake et al., 2011). Similarly, the MCD diet model of NASH had no impact on the mRNA or protein expression of UGT1A1 in rats, making it unlikely that alterations to the disposition of SN-38 glucuronide would be due to the effects of the disease on this enzyme(R. N. Hardwick, Fisher, Street, Canet, & Cherrington, 2012).

Uptake transporters may also have an effect on the disposition of SN-38. SN-38 is known to be transported by human OATP1B1, OATP1B3, and OATP2B1(Fujita, Saito, Nakanishi, & Tamai, 2015; Kalliokoski & Niemi, 2009), and rodent transporters OATP1B2, OATP2B1, and OATP1A4(Wang et al., 2016), though other transporters of organic anions may also be involved.   The MCD diet has been shown to alter the

mRNA and protein expression of various hepatic uptake transporters, including rat OATP1A1, OATP1A3, OATP1B2, and OATP2B1. Decreases have been observed in the mRNA expression of *Oatp1a1, 1a4, 1b2*, and *2b1*, while protein expression of Oatp1A1, 1B2, and 2B1 decreases and 1A4 does not change(Fisher et al., 2009). While mRNA and protein expression of transporters significantly impact drug disposition, the glycosylation status of these transporters will also play a role. The N-linked glycosylation of transporters has multiple functions, including protein maturation, stability, and function, and membrane bound proteins in particular rely on proper glycosylation for protein folding and trafficking to the appropriate membrane(Tannous, Brambilla, Hebert, & Molinari, 2015; Urquhart, Pang, & Hooper, 2005). In human NASH, it has been observed that genes involved in N-glycan synthesis are down-regulated, indicating a perturbation of N-linked glycosylation. This perturbation is reflected in the increase in unglycosylated OATP1B1, OATP1B3, OATP2B1, and NTCP protein found in human NASH patients(Clarke, Novak, Lake, Hardwick, & Cherrington, 2016). Disruption of normal glycosylation may be one mechanism by which NASH alters the function of transporter proteins.

Inter-individual variability can be accounted for in some cases by genetic polymorphisms; the function of hepatic transport proteins, however, can be affected not only by genetic variation, but also by disease state. NASH has been known to cause alterations in multiple efflux transporters, including MRP2 and MRP3. There is a trend towards increased efflux transporter expression in NASH in both the human disease and rodent MCD models (Canet et al., 2014; R. N. Hardwick et al., 2011). The interactions of these disease-induced alterations with genetic polymorphisms and their

functional consequences, however, have not been fully determined. Previous studies

have shown gene-by-environment interactions between NASH and genetic loss of

OATP transporters that affects the disposition of statins(Clarke et al., 2014). The

plasma and muscle concentrations of pravastatin were synergistically increased in

$Oatp1b2^{-/-}$ mice with NASH, indicating an increased risk for statin toxicity. Myopathy is

the major adverse effect of statin therapy, and it is known to be dose dependent and

related to plasma concentrations; this synergistic increase between the genotype and

disease indicates a potential at-risk patient group of those with OATP1B1

polymorphisms and NASH. We found that NASH causes an alteration to the normal

hepatobiliary efflux of SN-38 and SN-38G by perturbing the MRP2/MRP3 efflux pathway

through mislocalization of MRP2 and increased expression of MRP3. Compensation,

however, occurs in the form of upregulated BCRP, restoring sufficient biliary efflux and

leading to no significant alteration in SN-38 or SN-38G elimination in the MCD rodent

model. There is a significant gene-by-environment effect observed with the addition of

a genetic *Bcrp* knockout to the MCD diet, whereby removal of the compensatory BCRP

upregulation results in a sharp decrease in biliary elimination of both parent compound

and metabolite. There was no significant increase in plasma AUC over the observed

time points, though alteration to the plasma retention may only be observable at points

after the final 40 minute time point. Similarly, there was no statistically significant

difference in SN-38 or SN-38G retention in kidney or liver tissues when compared with

controls. We can therefore conclude that Bcrp plays a role in the disposition of SN-38

and SN-38G along with MRP2 and MRP3, and that its function as a compensatory

transporter is of increased importance in NASH. As BCRP can compensate for the loss

of other transporter function during NASH, disrupting its function can restrict the biliary excretion of SN-38 and SN-38G. Systemic retention of SN-38 may increase the risk of toxicity. It has been previously seen that decreased SN-38/SN-38G ratios in plasma are a predictor of the severity of neutropenia in irinotecan therapy, though not all irinotecan toxicity could be accounted for by UGT activity(Hirose et al., 2012; Iyer et al., 2002). Diminished efflux of SN-38G may also decrease the therapeutic efficacy of irinotecan by preventing the intestinal conversion of SN-38G to SN-38 and enterohepatic recycling.

These findings provide a mechanistic basis for variable response to irinotecan therapy and identify potential risk in vulnerable populations. NASH has only recently been identified as a factor in drug disposition and ADRs, and due to the invasive liver biopsy required for definitive diagnosis, susceptible patients may not be readily identified. Additionally, genetic variants of BCRP are relatively common, and the C421A variant can be found in 39% of Japanese and 30% of Caucasian populations, producing a transporter with a nonfunctional ATP-binding domain(Imai et al., 2002; Kobayashi et al., 2005). A less abundant variant, G34A, exists in 18% of Japanese populations, 6% of African-American populations, and 3% of Caucasian populations(Imai et al., 2002; Noguchi, Katayama, Mitsuhashi, & Sugimoto, 2009). Genetic variation in BCRP has also been shown to cause alterations to the pharmacokinetics and pharmacodynamics of drugs on its own(Mizuno, Fukudo, Terada, Kamba, & Nakamura, 2012; Zhang et al., 2006), and the combination of genetic polymorphisms and disease could potentially compound these changes as demonstrated herein with SN-38. With the increasing prevalence of NASH, the importance of phenoconversion in patients who also have genetic polymorphisms is significant. These data provide a possible mechanistic basis

for previously unidentified causes of variability and toxicity to BCRP substrates in NASH

patients.

Acknowledgements

DMD # 82081

Authorship Contributions

Participated in research design: Toth, Li, Dzierlenga, Clarke, Cherrington

Conducted experiments: Toth, Li, Dzierlenga, Clarke, Vildhede

Performed data analysis: Toth, Vildhede, Goedken

Wrote or contributed to the writing of the manuscript: Toth, Li, Clarke, Dzierlenga,

Vildhede, Goedken, Cherrington

23

References

Ali, I, Slizgi, J R, Kaullen, J D, Ivanovic, M, Niemi, M, Stewart, P W, … Brouwer, K L R. (2017). Transporter-Mediated Alterations in Patients With NASH Increase Systemic and Hepatic Exposure to an OATP and MRP2 Substrate. *Clin Pharmacol Ther*, 00(00), 1–8.

Bourgeois, F T, Shannon, M W, Valim, C, and Mandl, K. (2010). Adverse drug events in the outpatient setting: an 11-year national analysis. *Pharmacoepidemiol Drug Saf*, 19, 901–910.

Canet, M J, Hardwick, R N, Lake, A D, Dzierlenga, A L, Clarke, J D, and Cherrington, N J. (2014). Modeling Human Nonalcoholic Steatohepatitis-Associated Changes in Drug Transporter Expression Using Experimental Rodent Models. *Drug Metab Dispos*, 42(4), 586–595.

Chu, X, Kato, Y, Niinuma, K, Sudo, K, Hakusui, H, and Sugiyama, Y. (1997). Multispecific Organic Anion Transporter Is Responsible for the Biliary Excretion of the Camptothecin Derivative Irinotecan and its Metabolites in Rats 1. *J Pharmacol Exp Ther*, 281(1), 304–314.

Clarke, J D, Hardwick, R N, Lake, A D, Lickteig, A J, Goedken, M J, Klaassen, C D, and Cherrington, N J. (2014). Synergistic interaction between genetics and disease on pravastatin disposition. *J Hepatol*, 61(1), 139–147.

Clarke, J D, Novak, P, Lake, A D, Hardwick, R N, and Cherrington, N J. (2016). Impaired N- - linked glycosylation of uptake and efflux transporters in human non- - alcoholic fatty liver disease. *Metab Liver Dis*, 37(7), 1074–1081.

D'Esposito, F, Tattam, B N, Ramzan, I, and Murray, M. (2008). A liquid chromatography/electrospray ionization mass spectrometry (LC-MS/MS) assay for the determination of irinotecan (CPT-11) and its two major metabolites in human liver microsomal incubations and human plasma samples. *J Chromatogr B Anal Technol Biomed Life Sci*, 875(2), 522–530.

Dzierlenga, A L, Clarke, J D, Hargraves, T L, Ainslie, G R, Vanderah, T W, Paine, M F, and Cherrington, N J. (2015). Mechanistic Basis of Altered Morphine Disposition in Nonalcoholic Steatohepatitis. *J Pharmacol Exp Ther*, 352(3), 462–470.

Dzierlenga, A L, Clarke, J D, Klein, D M, Anumol, T, Snyder, S A, Li, H Y, and Cherrington, N. (2016). Biliary Elimination of Pemetrexed is Dependent on Mrp2 in Rats: Potential Mechanism of Variable Response in Nonalcoholic Steatohepatitis. *J Pharmacol Exp Ther* .

Etienne-Grimaldi, M C, Boyer, J C, Thomas, F, Quaranta, S, Picard, N, Loriot, M A, … Le Guellec, C. (2015). UGT1A1 genotype and irinotecan therapy: General review and implementation in routine practice. *Fundam Clin Pharmacol*, 29(3), 219–237.

Falcone, A, Ricci, S, Brunetti, I, Pfanner, E, Allegrine, G, Barbara, C, … Masi, G.

(2007). Phase III trial of infusional fluorouracil, leucovorin, oxaliplatin, and irinotecan (FOLFOXIRI) compared with infusional fluorouracil, leucovorin, and irinotecan (FOLFIRI) as first-line treatment for metastatic colorectal cancer: The gruppo oncologico nor. *J Clin Oncol*, 25(13), 1670–1676.

Ferslew, B C, Johnston, C K, Tsakalozou, E, Bridges, A S, Paine, M F, Jia, W, … Brouwer, K L R. (2015). Altered morphine glucuronide and bile acid disposition in patients with nonalcoholic steatohepatitis. *Clin Pharmacol Ther*, 97(4), 419–427.

Fisher, C D, Lickteig, A J, Augustine, L M, Oude Elferink, R P J, Besselsen, D G, Erickson, R P, and Cherrington, N J. (2009). Experimental non-alcoholic fatty liver disease results in decreased hepatic uptake transporter expression and function in rats. *Eur J Pharmacol*, 613(1), 119–127.

Fujita, D, Saito, Y, Nakanishi, T, and Tamai, I. (2015). Organic Anion Transporting Polypeptide (OATP)2B1 Contributes to Gastrointestinal Toxicity of Anticancer Drug SN-38, Active Metabolite of CPT-11. *Drug Metab Dispos*, 46(7).

Hardwick, R, Clarke, J D, Lake, A D, Canet, M, Anumol, T, Street, S, … Cherrington, N J. (2014). Increased Susceptibility to Methotrexate-Induced Toxicity in Nonalcoholic Steatohepatitis. *Toxicol Sci*, (520).

Hardwick, R N, Ferreira, D W, More, V R, Lake, A D, Lu, Z, Manautou, J E, … Cherrington, N J. (2013). Altered UDP-glucuronosyltransferase and sulfotransferase expression and function during progressive stages of human nonalcoholic fatty liver diseases. *Drug Metab Dispos*, 41(3), 554–561.

Hardwick, R N, Fisher, C D, Canet, M J, Scheffer, G L, and Cherrington, N J. (2011). Variations in ATP-Binding Cassette Transporter Regulation during the Progression of Human Nonalcoholic Fatty Liver Disease □ ABSTRACT : *Drug Metab Dispos*, 39(12), 2395–2402.

Hardwick, R N, Fisher, C D, Street, S M, Canet, M J, and Cherrington, N J. (2012). Molecular mechanism of altered ezetimibe disposition in nonalcoholic steatohepatitis. *Drug Metab Dispos*, 40(3), 450–460.

Hasegawa, Y, Ando, Y, Ando, M, Hashimoto, N, Imaizumi, K, and Shimokata, K. (2006). Pharmacogenetic approach for cancer treatment-tailored medicine in practice. *Ann N Y Acad Sci*, 1086, 223–232.

Hirose, K, Kozu, C, Yamashita, K, Maruo, E, Kitamura, M, Hasegawa, J, … Maeda, Y. (2012). Correlation between plasma concentration ratios of SN-38 glucuronide and sn-38 and neutropenia induction in patients with colorectal cancer and wild-type UGT1A1 gene. *Oncol Lett*, 3(3), 694–698.

Horikawa, M, Kato, Y, and Sugiyama, Y. (2002). Reduced Gastrointestinal Toxicity Following Inhibition of the Biliary Excretion of Irinotecan and Its Metabolites by Probenecid in Rats. *Pharm Res*, 19(9), 1345–1353.

Houghton, P J, Germain, G S, Harwood, F C, Schuetz, J D, Stewart, C F, Buchdunger, E, and Traxler, P. (2004). Imatinib Mesylate Is a Potent Inhibitor of the ABCG2 (BCRP) Transporter and Reverses Resistance to Topotecan and SN-38 in Vitro. *Cancer Res*, 64(7), 2333–2337.

Imai, Y, Nakane, M, Kage, K, Tsukahara, S, Ishikawa, E, Tsuruo, T, … Sugimoto, Y. (2002). C421A polymorphism in the human breast cancer resistance protein gene is associated with low expression of Q141K protein and low-level drug resistance. *Mol Cancer Ther*, 1(8), 611–616. Retrieved from http://www.ncbi.nlm.nih.gov/pubmed/12479221

Iusuf, D, Ludwig, M, Elbatsh, A, van Esch, A, van de Steeg, E, Wagenaar, E, … Schinkel, A H. (2014). OATP1A/1B Transporters Affect Irinotecan and SN-38 Pharmacokinetics and Carboxylesterase Expression in Knockout and Humanized Transgenic Mice. *Mol Cancer Ther*, 13(2), 492–503.

Iyer, L, Das, S, Janisch, L, Wen, M, Ramírez, J, Karrison, T, … Ratain, M J. (2002). UGT1A1*28 polymorphism as a determinant of irinotecan disposition and toxicity. *Pharmacogenomics J*, 2(1), 43–47.

Kalliokoski, A, and Niemi, M. (2009). Impact of OATP transporters on pharmacokinetics. *Br J Pharmacol*, 158, 693–705.

Kato, Y, Suzuki, H, and Sugiyama, Y. (2002). Toxicological implications of hepatobiliary transporters. *Toxicology*, 181–182, 287–290.

Kawabata, S, Oka, M, Shiozawa, K, Tsukamoto, K, Nakatomi, K, Soda, H, … Kohno, S. (2001). Breast cancer resistance protein directly confers SN-38 resistance of lung cancer cells. *Biochem Biophys Res Commun*, 280(5), 1216–1223.

Khan, S, Ahmad, A, Guo, W, Wang, Y F, Abu-Qare, A, and Ahmad, I. (2005). A simple and sensitive LC/MS/MS assay for 7-ethyl-10-hydroxycamptothecin (SN-38) in mouse plasma and tissues: Application to pharmacokinetic study of liposome entrapped SN-38 (LE-SN38). *J Pharm Biomed Anal*, 37(1), 135–142.

Kleiner, D E, Brunt, E M, Van Natta, M, Behling, C, Contos, M J, Cummings, O W, … Sanyal, A J. (2005). Design and validation of a histological scoring system for nonalcoholic fatty liver disease. *Hepatology*, 41(6), 1313–1321.

Kobayashi, D, Ieiri, I, Hirota, T, Takane, H, Maegawa, S, Kigawa, J, … Sugiyama, Y. (2005). Functional assessment of ABCG2 (BCRP) gene polymorphisms to protein expression in human placenta. *Drug Metab Dispos*, 33(1), 94–101.

Köck, K, and Brouwer, K L R. (2012). A Perspective on Efflux Transport Proteins in the Liver. *Clin Pharmacol Ther*, 92(5), 599–612.

Kroetz, D L. (2006). Role for drug transporters beyond tumor resistance: Hepatic functional imaging and genotyping of multidrug resistance transporters for the prediction of irinotecan toxicity. *J Clin Oncol*, 24(26), 4225–4227.

Lake, A D, Novak, P, Fisher, C D, Jackson, J P, Hardwick, R N, Billheimer, D D, … Cherrington, N J. (2011). Analysis of global and absorption, distribution, metabolism, and elimination gene expression in the progressive stages of human nonalcoholic fatty liver disease. *Drug Metab Dispos*.

Lal, S, Wong, Z W, Sandanaraj, E, Xiang, X, Ang, P C S, Lee, E J D, and Chowbay, B. (2008). Influence of ABCB1 and ABCG2 polymorphisms on doxorubicin disposition in Asian breast cancer patients. *Cancer Sci*, 99(4), 816–823.

Lara, P N, Natale, R, Crowley, J, Lenz, H J, Redman, M W, Carleton, J E, … Gandara, D R. (2009). Phase III trial of irinotecan/cisplatin compared with etoposide/cisplatin in extensive-stage small-cell lung cancer: Clinical and pharmacogenomic results from SWOG S0124. *J Clin Oncol*, 27(15), 2530–2535.

Liu, X, Cheng, D, Kuang, Q, Liu, G, and Xu, W. (2014). Association of UGT1A1*28 polymorphisms with irinotecan-induced toxicities in colorectal cancer: A meta-analysis in Caucasians. *Pharmacogenomics J*, 14(2), 120–129.

Marra, F, Gastaldelli, A, Svegliati Baroni, G, Tell, G, and Tiribelli, C. (2008). Molecular basis and mechanisms of progression of non-alcoholic steatohepatitis. *Trends Mol Med*, 14(2), 72–81.

Mizuno, T, Fukudo, M, Terada, T, Kamba, T, and Nakamura, E. (2012). Impact of Genetic Variation in Breast Cancer Resistance Protein. *Drug Metab Pharmacokinet*, 27(6), 631–639.

Noguchi, K, Katayama, K, Mitsuhashi, J, and Sugimoto, Y. (2009). Functions of the breast cancer resistance protein (BCRP/ABCG2) in chemotherapy. *Adv Drug Deliv Rev*, 61(1), 26–33.

Sadée, W, and Dai, Z. (2005). Pharmacogenetics/genomics and personalized medicine. *Hum Mol Genet*, 14(SUPPL. 2), 207–214.

Siegel, R, Desantis, C, and Jemal, A. (2014). Colorectal Cancer Statistics, 2014. *CA Cancer J Clin*, 64(1), 104–117.

Sparreboom, A, Gelderblom, H, Marsh, S, Ahluwalia, R, Obach, R, Principe, P, … McLeod, H L. (2004). Diflomotecan pharmacokinetics in relation to ABCG2 421C>A genotype. *Clin Pharmacol Ther*, 76(1), 38–44.

Stausberg, J. (2014). International prevalence of adverse drug events in hospitals: an analysis of routine data from England, Germany, and the USA. *BMC Health Serv Res*, 14(1), 125.

Tannous, A, Brambilla, G, Hebert, D N, and Molinari, M. (2015). N-linked sugar-regulated protein folding and quality control in the ER. *Semin Cell Dev Biol*, 41, 79–89.

Tuy, H D, Shiomi, H, Mukaisho, K I, Naka, S, Shimizu, T, Sonoda, H, … Tani, T. (2016). ABCG2 expression in colorectal adenocarcinomas may predict resistance to

27

irinotecan. *Oncol Lett*, 12(4), 2752–2760.

Urquhart, P, Pang, S, and Hooper, N M. (2005). N-glycans as apical targeting signals in polarized epithelial cells. *Biochem Soc Symp*, 72, 39–45.

Wang, X, Rao, Z, Qin, H, Zhang, G, Ma, Y, Jin, Y, and Han, M. (2016). Effect of hesperidin on the pharmacokinetics of CPT-11 and its active metabolite SN-38 by regulating hepatic Mrp2 in rats, 432(July), 421–432.

Yee, S W, Brackman, D J, Ennis, E A, Sugiyama, Y, Kamdem, L K, Blanchard, R, … Giacomini, K M. (2018). Influence of Transporter Polymorphisms on Drug Disposition and Response : A Perspective From the International Transporter Consortium. *Clin Pharmacol Ther*, 00(00), 1–15.

Younossi, Z M, Koenig, A B, Abdelatif, D, Fazel, Y, Henry, L, and Wymer, M. (2016). Global epidemiology of nonalcoholic fatty liver disease—Meta-analytic assessment of prevalence, incidence, and outcomes. *Hepatology*, 64(1), 73–84.

Zhang, W, Yu, B N, He, Y J, Fan, L, Li, Q, Liu, Z Q, … Zhou, H H. (2006). Role of BCRP 421C>A polymorphism on rosuvastatin pharmacokinetics in healthy Chinese males. *Clin Chim Acta*, 373(1–2), 99–103.

DMD # 82081

Footnotes

Legends for Figures

Figure 1. Liver histopathology of control and MCD-diet rats. Hemotoxylin and eosin stained liver sections of control rats and rats fed 8 weeks of MCD diet, wild-type and Bcrp knockouts. Hallmark characteristics of NASH were found in MCD rats, while control group animals showed no signs of NASH pathology. Original magnification, 40x. 2-way ANOVA, *$P \le 0.05$, ** $P \le 0.01$, *** $P \le 0.001$, n=3, n=4 (KO-MCD) .

Figure 2. Effects of MCD diet on systemic exposure of SN-38 and SN-38G. Plasma concentrations were taken over 40 minutes after intravenous infusion of 0.8mg/kg SN-38. Graphs represent mean ± S.D., n=3, n=4 (KO-MCD)

Figure 3. Effects of MCD diet on biliary excretion of SN-38 and SN-38G. Bile concentrations were taken over 45 minutes after intravenous infusion of 0.8mg/kg SN-38. Graphs represent mean ± S.D. 2-way ANOVA, *$P \le 0.05$, n=3, n=4 (KO-MCD) .

Figure 4. Alterations of Mrp2 and Mrp3 protein expression in MCD diet. Relative protein expression of (A) Mrp2 and (B) Mrp3 between control and MCD groups. (C) Relative protein expression was determined by immunoblot analysis. Graphs represent mean ± S.D. 2-way ANOVA, *$P \le 0.05$, n=3, n=4 (KO-MCD) .

Figure 5. Mislocalization of Mrp2 in MCD diet. Protein localization of Mrp2 was visualized by immunohistochemistry in paraffin-embedded liver tissue of controls and MCD groups. Representative images were taken at 100x magnification.

Figure 6. Alterations of Bcrp protein and mRNA expression during MCD diet. (A) mRNA expression was determined by qRT-PCR analysis and fold change was determined using the delta-delta C_T method. Protein expression was determined by proteomic analysis using LC-MS/MS. Graphs represent mean ± S.D. 2-way ANOVA, *$P \le 0.05$ and ***$P \le 0.01$., n=3, n=4 (KO-MCD). (B) Representative chromatograms of WT-C, WT-MCD, and KO groups. Left chromatogram depicts native protein concentration and right chromatogram depicts internal standard peptide.

Figures

Figure 1

Figure 2

Plasma SN-38
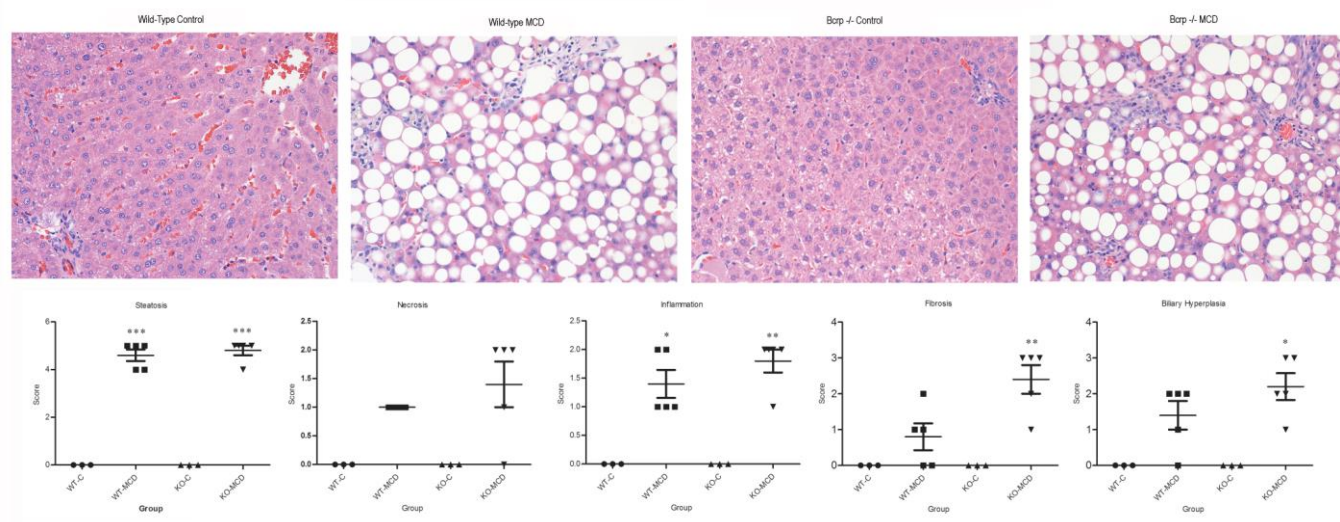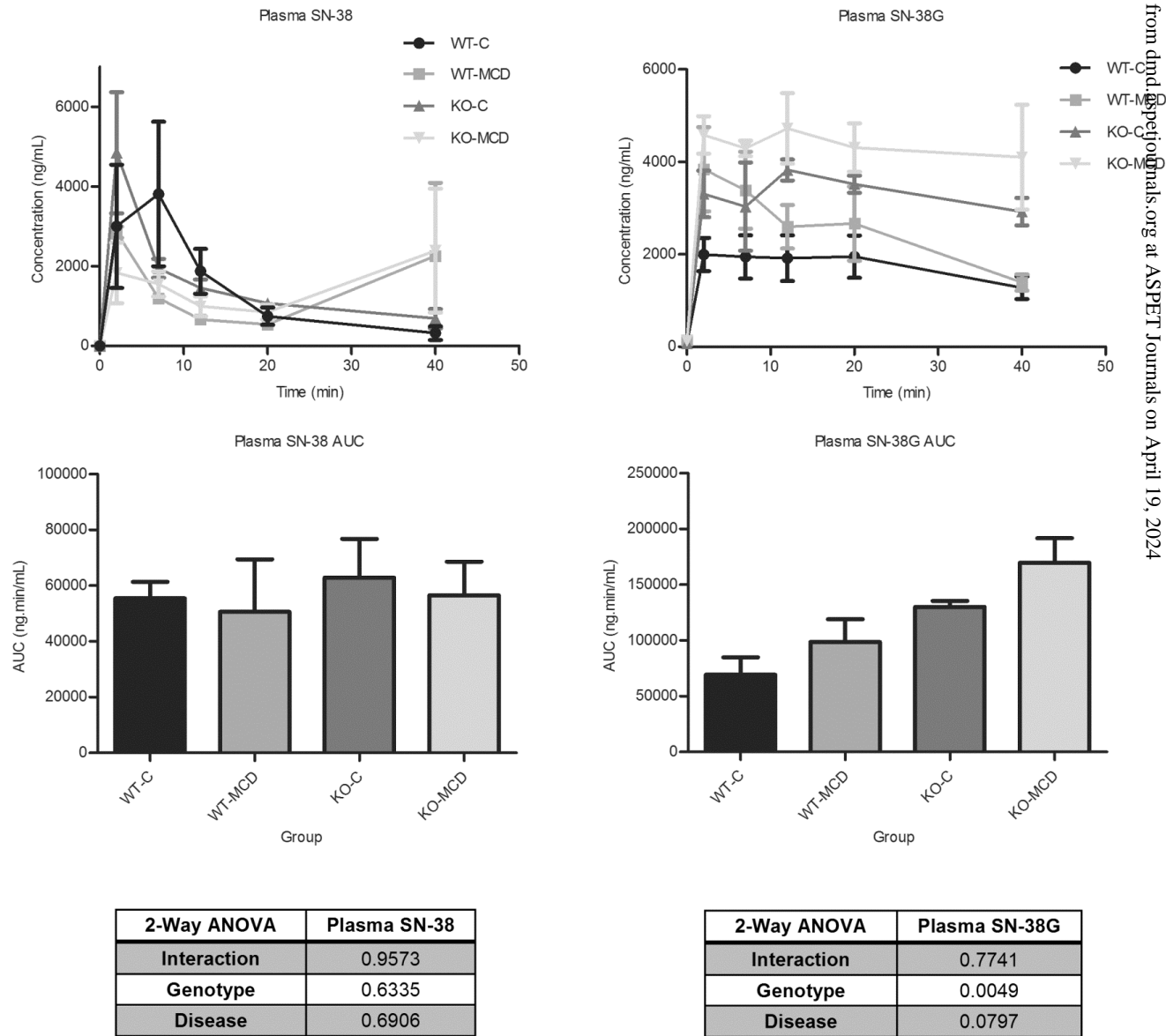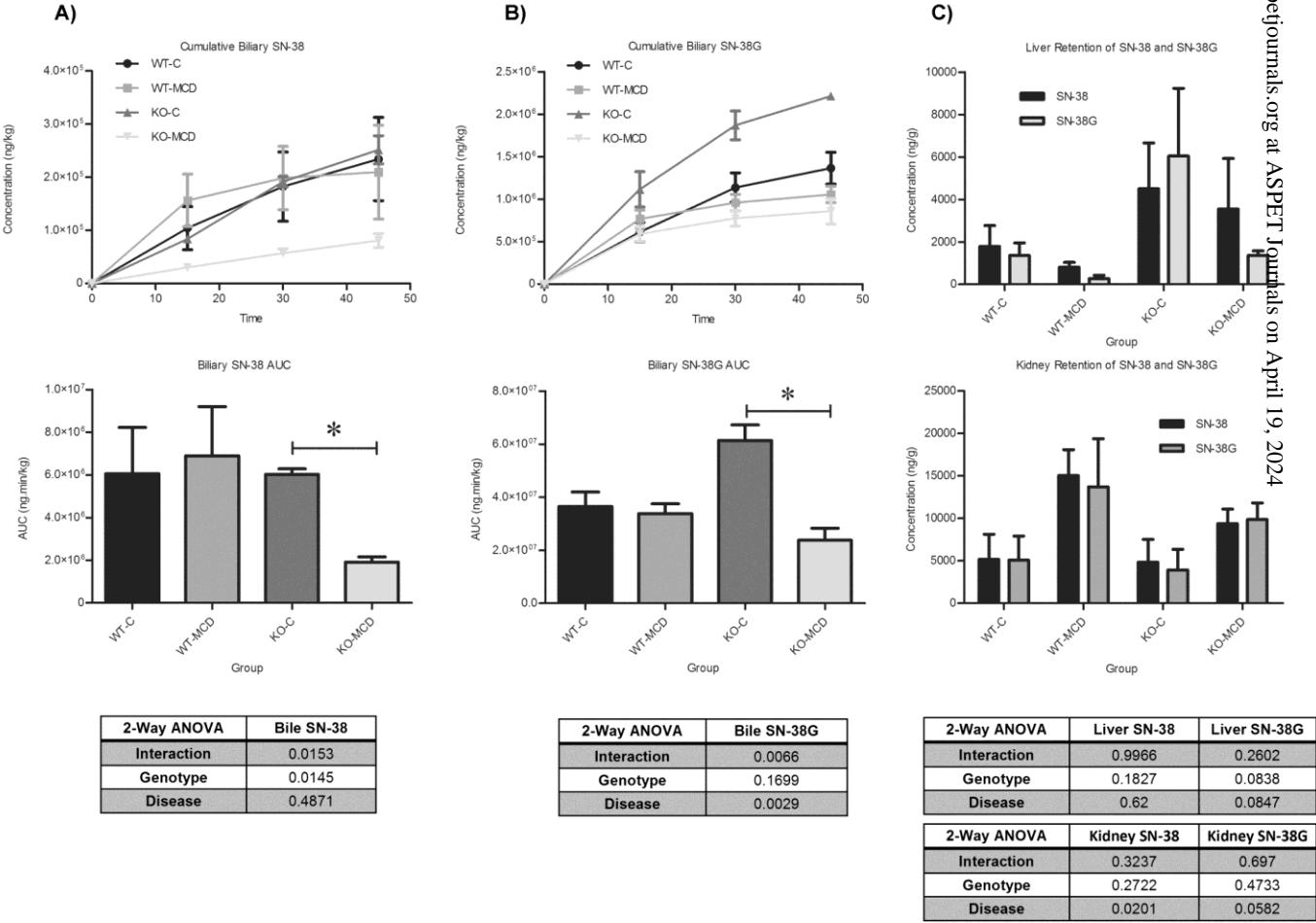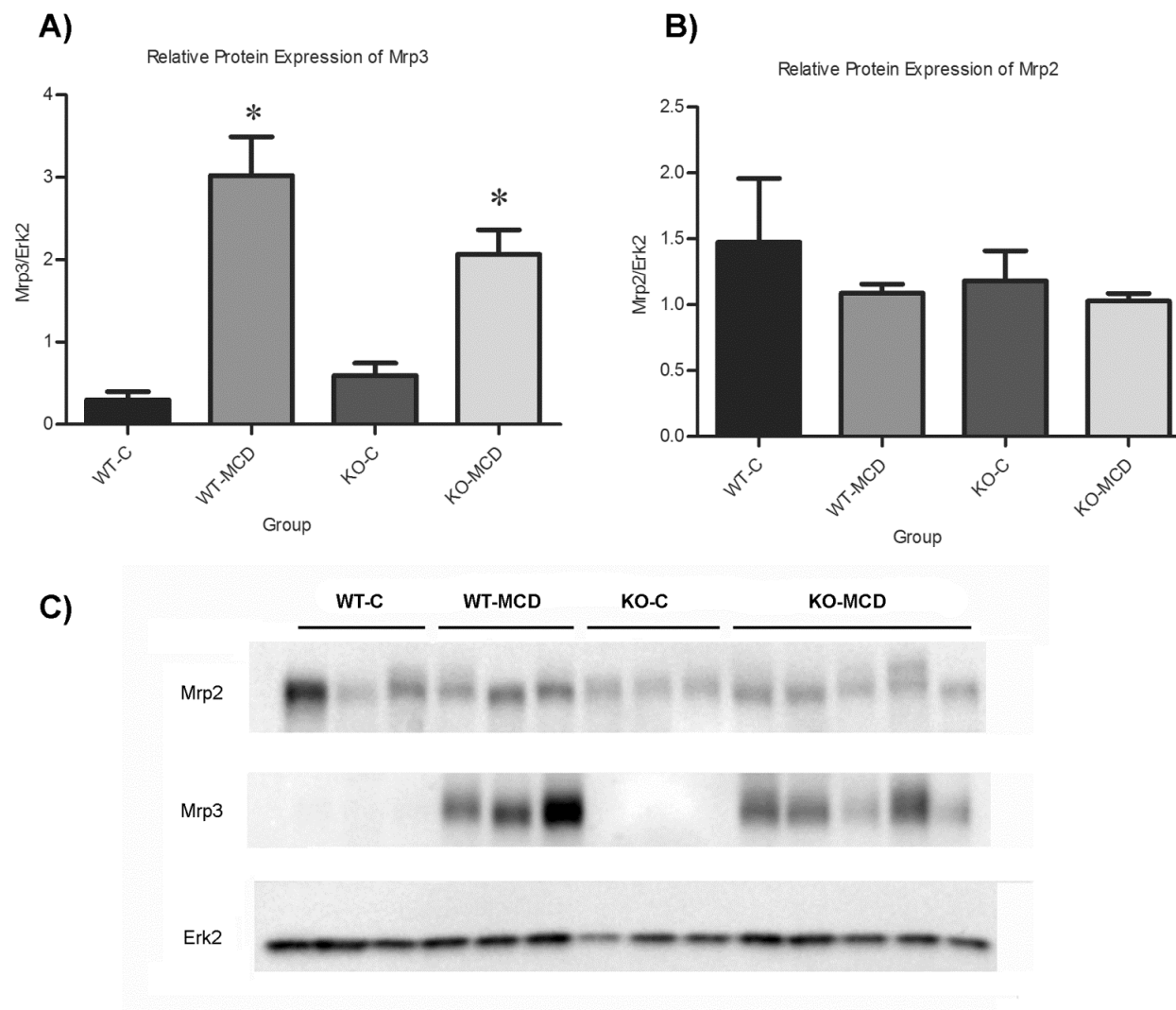
2-Way ANOVA	Plasma SN-38
Interaction	0.9573
Genotype	0.6335
Disease	0.6906

Plasma SN-38G

2-Way ANOVA	Plasma SN-38G
Interaction	0.7741
Genotype	0.0049
Disease	0.0797

Figure 3

A)

Cumulative Biliary SN-38

Legend: WT-C, WT-MCD, KO-C, KO-MCD

Biliary SN-38 AUC

2-Way ANOVA	Bile SN-38
Interaction	0.0153
Genotype	0.0145
Disease	0.4871

B)

Cumulative Biliary SN-38G

Legend: WT-C, WT-MCD, KO-C, KO-MCD

Biliary SN-38G AUC

2-Way ANOVA	Bile SN-38G
Interaction	0.0066
Genotype	0.1699
Disease	0.0029

C)

Liver Retention of SN-38 and SN-38G

Legend: SN-38, SN-38G

Kidney Retention of SN-38 and SN-38G

Legend: SN-38, SN-38G

2-Way ANOVA	Liver SN-38	Liver SN-38G
Interaction	0.9966	0.2602
Genotype	0.1827	0.0838
Disease	0.62	0.0847

2-Way ANOVA	Kidney SN-38	Kidney SN-38G
Interaction	0.3237	0.697
Genotype	0.2722	0.4733
Disease	0.0201	0.0582

Figure 4

A)

Relative Protein Expression of Mrp3

B)

Relative Protein Expression of Mrp2

C)

Figure 5

Wild-Type Control

Wild-Type MCD

Bcrp -/- Control

Bcrp -/- MCD

Figure 6

A)

Relative mRNA Expression of Bcrp

Relative Protein Expression of Bcrp

B)